The Journal of Nutrition
Nutrient Physiology, Metabolism, and Nutrient-Nutrient Interactions

Production of 1-Carbon Units from Glycine Is Extensive in Healthy Men and Women[1,2]

Yvonne Lamers,[3] Jerry Williamson,[3] Douglas W. Theriaque,[4] Jonathan J. Shuster,[4,5] Lesa R. Gilbert,[6] Christine Keeling,[6] Peter W. Stacpoole,[4,6,7] and Jesse F. Gregory III[3]*

[3]Food Science and Human Nutrition Department, Institute of Food and Agricultural Sciences, [4]General Clinical Research Center, [5]Division of Biostatistics, Department of Epidemiology and Health Policy Research, [6]Division of Endocrinology and Metabolism, Department of Medicine, and [7]Department of Biochemistry and Molecular Biology, College of Medicine, University of Florida, Gainesville, FL 32611-0370

Abstract

Glycine undergoes decarboxylation in the glycine cleavage system (GCS) to yield CO_2, NH_3, and a 1-carbon unit. CO_2 also can be generated from the 2-carbon of glycine by 10-formyltetrahydrofolate-dehydrogenase and, after glycine-to-serine conversion by serine hydroxymethyltransferase, from the tricarboxylic acid cycle. To evaluate the relative fates of glycine carbons in CO_2 generation in healthy volunteers (3 male, 3 female, aged 21–26 y), primed, constant infusions were conducted using 9.26 μmol·h^{-1}·kg^{-1} of [1,2-^{13}C]glycine and 1.87 μmol·h^{-1}·kg^{-1} of [5,5,5-$^{2}H_3$]leucine, followed by an infusion protocol using [1-^{13}C]glycine as the glycine tracer. The time period between the infusion protocols was >6 mo. In vivo rates of whole-body glycine and leucine flux were nearly identical in protocols with [1,2-^{13}C]glycine and [5,5,5-$^{2}H_3$]leucine and with [1-^{13}C]glycine and [5,5,5-$^{2}H_3$]leucine tracers, which showed high reproducibility between the tracer protocols. Using the [1-^{13}C]glycine tracer, breath CO_2 data showed a total rate of glycine decarboxylation of 96 ± 8 μmol·h^{-1}·kg^{-1}, which was 22 ± 3% of whole-body glycine flux. In contrast, infusion of [1,2-^{13}C]glycine yielded a glycine-to-CO_2 flux of 146 ± 37 μmol·h^{-1}·kg^{-1} ($P = 0.026$). By difference, this implies a rate of CO_2 formation from the glycine 2-carbon of 51 ± 40 μmol·h^{-1}·kg^{-1}, which accounts for ~35% of the total CO_2 generated in glycine catabolism. These findings also indicate that ~65% of the CO_2 generation from glycine occurs by decarboxylation, primarily from the GCS. Further, these results suggest that the GCS is responsible for the entry of 5,10-methylenetetrahydrofolate into 1-carbon metabolism at a very high rate (~96 μmol·h^{-1}·kg^{-1}), which is ~20 times the demand for methyl groups for homocysteine remethylation. J. Nutr. 139: 666–671, 2009.

Introduction

Glycine is a precursor for the synthesis of purines, protein, glutathione, and 1-carbon units in folate-dependent 1-carbon metabolism. Through the mitochondrial glycine cleavage system (GCS),[8] glycine undergoes decarboxylation to yield CO_2, ammonia, and a 1-carbon unit in the form of 5,10-methylenetetrahydrofolate (methyleneTHF) (1). This 1-carbon unit from glycine is used in reactions including nucleotide synthesis, regeneration of methionine from homocysteine, and methylation of many biological compounds. One-carbon metabolism is linked to the transsulfuration pathway in which homocysteine undergoes vitamin B-6–dependent catabolism leading to cysteine, whose availability governs the formation of the antioxidant glutathione. Nutritional or genetic conditions that impair 1-carbon metabolism are associated with elevation in plasma homocysteine concentration and increased risk of vascular disease (2).

In addition to glycine cleavage, CO_2 can be formed from glycine carbons through mitochondrial and cytosolic pathways of folate or pyruvate metabolism in healthy individuals (**Fig. 1**). MethyleneTHF synthesized via GCS can be enzymatically oxidized to 10-formylTHF by methyleneTHF dehydrogenase. 10-FormylTHF dehydrogenase converts 10-formylTHF to tetrahydrofolate (THF) and CO_2, which appears to be a mechanism of achieving a regeneration of THF and regulating 1-carbon pools (3). Glycine and serine are interconvertible through mitochondrial and cytosolic serine hydroxymethyltransferase (SHMT). We previously showed that glycine-to-serine conversion via SHMT accounts for ~41% of whole-body glycine flux, a sum of mitochondrial and cytoplasmic processes (4). Serine synthesis with a GCS-derived 1-carbon unit (Fig. 1, left) accounted for 46% of total serine synthesis rate (4). Serine dehydratase transforms

[1] Supported by the NIH grant DK072398 and General Clinical Research Center grant M01-RR00082.
[2] Author disclosures: Y. Lamers, J. Williamson, D. W. Theriaque, J. J. Shuster, L. R. Gilbert, C. Keeling, P. W. Stacpoole, and J. F. Gregory, no conflicts of interest.
[8] Abbreviations used: AUC, area under the curve; Ep, plateau enrichment; 10-formylTHF, 10-formyltetrahydrofolate; GCRC, General Clinical Research Center; GCS, glycine cleavage system; I, infusion rate; methyleneTHF, 5,10-methylenetetrahydrofolate; PLP, pyridoxal 5′-phosphate; Q, a measurement of flux; SHMT, serine hydroxymethyltransferase; TCA, tricarboxylic acid; THF, tetrahydrofolate; VCO_2, rate of CO_2 production.
* To whom correspondence should be addressed. E-mail: jfgy@ufl.edu.

Manuscript received December 12, 2008. Initial review completed January 14, 2009. Revision accepted January 31, 2009.
First published online February 25, 2009; doi:10.3945/jn.108.103580.

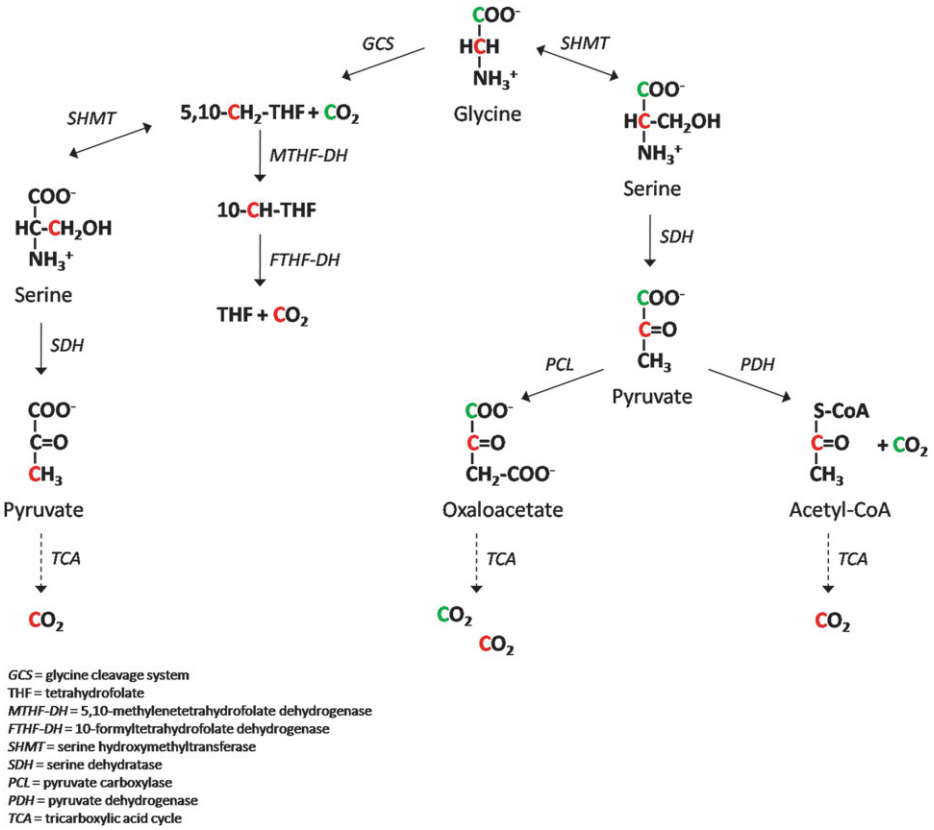

FIGURE 1 Schematic of possible fates of glycine carbons as CO_2.

serine to pyruvate that enters the tricarboxylic acid (TCA) cycle either as oxaloacetate or acetyl-CoA. The carbons of serine, following conversion to pyruvate, can be converted to CO_2 via the pyruvate dehydrogenase reaction and metabolism of the resulting acetyl-CoA and through the TCA cycle. Alternatively, serine carbons (via pyruvate) also can be converted to CO_2 after the formation of oxaloacetate by pyruvate carboxylase, followed by metabolism in the TCA cycle.

With the use of stable isotope tracer protocols, we aimed to quantify postprandial rates of in vivo glycine turnover and the relative fates of glycine carbons in CO_2 generation in healthy, adequately nourished men and women. The tracer protocols included primed, constant infusions of [1,2-^{13}C]glycine or [1-^{13}C]glycine and [$^{2}H_3$]leucine with a time period between both protocols of >6 mo. [$^{2}H_3$]Leucine was included to determine any changes in protein turnover (5,6). The results of whole-body glycine flux after infusion with [1,2-^{13}C]glycine and [$^{2}H_3$]leucine tracers were part of a recently published protocol (7). Measurement of breath $^{13}CO_2$ enrichment (8) was used for quantification of the fates of glycine carbons with respect to the generation of CO_2. Formation of CO_2 from the [1-^{13}C]glycine tracer is hypothesized to occur primarily from glycine decarboxylation through the GCS. The difference between CO_2 formation after infusion with [1,2-^{13}C]glycine and CO_2 production from [1-^{13}C]glycine tracer infusion would account for the fate of the 2-carbon of glycine as CO_2.

Methods

Materials

[1,2-^{13}C]Glycine, [1-^{13}C]glycine, L-[5,5,5-$^{2}H_3$]leucine, and sodium [^{13}C]bicarbonate were purchased from Cambridge Isotopes Laboratories. Parenteral solutions were prepared in isotonic saline, filter sterilized and analyzed to ensure lack of pyrogenicity and microbial contamination.

Human participants

Adult male and nonpregnant female participants underwent a physical examination and were screened by standard clinical measures of hematological, renal, hepatic, and thyroid function before each infusion protocol. Medical history, dietary habits, and demographic data were assessed by a questionnaire. All participants met the following inclusion criteria: age between 20 and 40 y, no history of gastrointestinal surgery, abnormal kidney, or thyroid function, or any other chronic disease; no smoking or chronic drug use or alcoholism; no vitamin, amino acid, or protein supplementation; no chronic consumption of a high-protein diet; and a BMI of <28 kg/m^2. Adequate nutritional status for folate and vitamins B-12 and B-6 was defined as serum folate >7 nmol/L, serum vitamin B-12 >200 pmol/L, and plasma pyridoxal 5′-phosphate (PLP) >30 nmol/L, respectively, and plasma total homocysteine concentration <12 μmol/L. All participants gave written informed consent. The University of Florida Institutional Review Board and the General Clinical Research Center (GCRC) Scientific Advisory Committee approved this protocol.

Dietary treatment

All meals were prepared by the Bionutrition Unit of the GCRC. Participants consumed nutritionally adequate meals with standardized composition for 2 d prior to the infusion day to minimize dietary variation immediately prior to the study.

Analytical methods

Screening measurements. The analytical procedures used for data collection are as described previously (4). Serum folate and vitamin B-12 were analyzed with the use of a commercial chemiluminescence-based assay (Elecsys, Roche Diagnostics). The plasma PLP concentration was measured as the semicarbazone-derivative by reverse-phase HPLC with

fluorescence detection (9). After incubation with the reducing agent tris(2-carboxyethyl)phosphine before protein precipitation, the plasma total homocysteine concentration was measured as the ammonium 7-fluorobenzo-2-oxa-1,3-diazole-4-sulfonate derivative by reverse-phase HPLC with fluorescence detection (10).

GC-MS analysis of amino acid isotopic enrichment. Plasma free amino acids were isolated, derivatized, and analyzed as previously described (6). The *N*-heptafluorobutyramide-n-propyl ester derivatives were dried, dissolved in ethyl acetate, and stored at −20°C until analysis. Isotopic enrichment was determined by negative chemical ionization GC-MS with the use of a Thermo-Finnigan DSQ GC-MS and a 30-m poly (5% diphenyl and 95% dimethylsiloxane) fused silica capillary column (Equity 5, Supelco). The relative abundance of specific ions was determined by selected-ion monitoring at the following mass:charge ratios: glycine (293–295) and leucine (349–352). Isotopic enrichments are expressed as molar ratios of labeled to nonlabeled isotopomers after correction for the natural abundance of stable isotopes essentially as performed by Storch et al. (11).

Breath CO_2. For determination of the isotopic enrichment of breath $^{13}CO_2$, samples were collected in Exetainer tubes provided by Metabolic Solutions and shipped to Metabolic Solutions for isotope ratio-MS analysis. Total CO_2 production rate (VCO_2) was determined with the use of a metabolic cart (TrueMax 2400; ParvoMedics). Measurements were taken at 30-s intervals for ~5 min until 4 consecutive time points differed by no more than ±0.01 L/min.

Infusion protocol

The infusion protocol has been previously reported (4) and was identical for both interventions except for the glycine tracer used. The time period between both protocols was >6 mo. Participants were admitted to the GCRC on the evening before the infusion protocol and consumed no food and drinks, except water, between 2100 and initiation of the infusion. On the morning of the infusion, an angiocatheter was inserted in the antecubital vein of each arm; 1 for the tracer infusion and 1 for blood collection. Fasting blood samples were taken 2 h before infusion (at ~0700) for measurement of folate and vitamin B-12 and B-6 status and plasma total homocysteine concentrations. Infusions were initiated at ~0900 with a 5 min, ~20 mL priming dose that delivered 9.26 μmol/kg [1,2-^{13}C]glycine or 9.26 μmol/kg [1-^{13}C]glycine and 1.87 μmol/kg [5,5,5-$^{2}H_3$]leucine, respectively, along with a simultaneous priming dose of 2.15 μmol/kg of $NaH^{13}CO_3$. The 9-h constant infusion followed immediately after the priming dose and delivered ~20 mL/h infusion solution that contained 9.26 μmol/kg [1,2-^{13}C]glycine or 9.26 μmol/kg [1-^{13}C]glycine and 1.87 μmol/kg [5,5,5-$^{2}H_3$]leucine.

Blood samples were taken at 0, 0.5, 1, 1.5, 2, 2.5, 3, 4, 5, 6, 7.5, and 9 h of the infusion. These samples were placed immediately on ice and were centrifuged within 15 min after the blood draw at 1500 × *g* (10 min at 4°C). Plasma was stored in microcentrifuge tubes at −80°C.

To measure $^{13}CO_2$ production, breath samples were collected into Exetainer tubes at times 0, 1, 2, 3, 4, and 6 h of infusion in both protocols and additionally at 5 h of infusion in the protocol using [1,2-^{13}C]glycine and at 7.5 and 9 h of infusion in the protocol using [1-^{13}C]glycine. Measurements of the total VCO_2 were conducted at 0, 2, 4, 6, and 8 h of infusion. Starting 2 h before infusion after drawing of the fasting blood sample, the participants received hourly a nutritive formula to maintain a fed state (11). This formula provided an intake of energy and a balanced pattern of amino acids at a rate based on requirements of 0.8 g protein·kg^{-1}·d^{-1} [30 and 31 kcal·kg^{-1}·d^{-1} (126 and 130 kJ·kg^{-1}·d^{-1}) for women and men, respectively], which equals an hourly protein dose of ~0.03 g/kg with 1.25 and 1.30 kcal·kg^{-1}·d^{-1} (5.23 and 5.44 kJ·kg^{-1}·d^{-1}) for women and men, respectively.

Kinetic principles and analysis

As previously described (4), the combined use of [1,2-^{13}C]glycine or [1-^{13}C]glycine and [$^{2}H_3$]leucine permitted the determination of the kinetics of whole-body glycine turnover, the rate of glycine decarboxylation, and its role as a source of 1-carbon units in 1-carbon metabolism. [$^{2}H_3$]Leucine is included to evaluate any effects on protein turnover (5,6). During the decarboxylation and catabolism of a glycine tracer via the GCS, the original glycine ^{13}C-labeled carbon at the 2-carbon position is transferred to THF to yield methyleneTHF. The major focus of the study reported here was to determine the quantitative aspects of the different fates of glycine carbons as CO_2 through GCS and folate cycle (Fig. 1).

The plateau enrichment (Ep) of all infused amino acid tracers was calculated as the mean of the isotopic enrichment for the ~1.5–9-h time points for the infused [$^{13}C_2$]glycine, [$^{13}C_1$]glycine, and [$^{2}H_3$]leucine tracers. The Ep of breath $^{13}CO_2$ was approximated by fitting enrichment data to a single exponential curve defined by the equation

$$E_t = E_f(1-e^{-kt}). \quad (1)$$

In this equation, E_t is the enrichment at time t (h), whereas E_f and k are the enrichment at infinity (i.e. Ep) and rate constant (h^{-1}) from the fitted curve, respectively (12). Data were fit to a single regression exponential equation with the use of SigmaPlot 2002 (for Windows version 8.02).

Steady-state kinetics of amino acid tracers were calculated using standard equations (13), including correction for overestimation of intracellular enrichment from plasma enrichment data (11–13), as discussed below. The flux of an amino acid is the rate of appearance of that amino acid from endogenous production (de novo synthesis and protein breakdown), absorption, and the tracer infusion, and is calculated from the Ep of the corresponding amino acid tracer. Specifically, the flux (Q) of leucine (Q_{Leu}) in the plasma pool is calculated as:

$$Q_{Leu} = I_{Leu} \cdot [(E_{Leu})/(Ep_{Leu})-1], \quad (2)$$

where I_{Leu} is the [$^{2}H_3$]leucine infusion rate, E_{Leu} is the enrichment of the [$^{2}H_3$]leucine tracer and Ep_{Leu} is the Ep of [$^{2}H_3$]leucine in plasma. The Ep of plasma leucine was not corrected for overestimation of intracellular enrichment, consistent with previous studies using leucine flux as a relative indicator of protein turnover (5,14,15).

Glycine flux (Q_{Gly}) was calculated from plasma [1,2-^{13}C]glycine enrichment after correcting for the overestimation of the intracellular [1,2-^{13}C]glycine enrichment that occurs when the plasma Ep of the glycine tracer is used. This prediction of intracellular [1,2-^{13}C]glycine enrichment (Ep'$_{Gly}$) was accomplished by multiplying the observed plasma [1,2-^{13}C]glycine enrichment by a correction factor of 0.4 derived from previous glycine tracer infusion studies in humans (16,17). The same calculation was done for the [1-^{13}C]glycine tracer.

$$Q_{Gly} = I_{Gly} \cdot [(E_{Gly})/(Ep'_{Gly})-1] \quad (3)$$

The rate of production of $^{13}CO_2$ provided a direct measurement of the whole-body flux of the decarboxylation of the glycine tracer. This was measured in standard fashion as in amino acid oxidation studies (11,18). In this procedure, the rate of $^{13}CO_2$ release ($V^{13}CO_2$; in units of μmol·h^{-1}·kg^{-1} body weight) and the rate of glycine catabolism via decarboxylation (C_{Gly}; μmol·h^{-1}·kg^{-1} body weight) were calculated as follows:

$$V^{13}CO_2 = E^{13}CO_2 \cdot VCO_2/0.81 \cdot 1/W, \quad (4)$$

where $E^{13}CO_2$ is breath CO_2 enrichment at plateau, VCO_2 is the rate of total CO_2 production, 0.81 is the assumed fraction of CO_2 release from the body pool of bicarbonate, and W is body weight (18).

$$C_{Gly} = V^{13}CO_2 \cdot [(1/Ep'_{Gly})-(1/Ei_{Gly})], \quad (5)$$

where Ep'$_{Gly}$ is the Ep of plasma [$^{13}C_2$]glycine corrected for intracellular overestimation and Ei_{Gly} is the enrichment of the infused glycine tracer.

The fraction of Q_{Gly} occurring via glycine decarboxylation was calculated as

$$F_{GCS} = C_{Gly}/Q_{Gly}. \quad (6)$$

Statistical analysis

Descriptive statistics are presented as means and SD. The 2 primary outcome measurements were the yield of breath $^{13}CO_2$ enrichment after [1,2-^{13}C]glycine and [1-^{13}C]glycine infusion. The primary dependent variable for each of these outcomes was constructed as the area under the

curve (AUC) based on the trapezoidal rule for times 1, 2, 3, 4, and 6 h postinfusion, the times where both protocols collected the same information, dividing this result by 6 to obtain a mean value for the 6 h. Differences between infusion trials differing in the glycine tracer employed were tested via 2-sided paired *t* tests with differences considered significant at $P < 0.05$. All other statistical comparisons, including time-specific comparisons of the 2 primary outcome measures, were conducted in the same manner. The target sample size was 10 participants, the number of participants from the [1,2-$^{13}C_2$]glycine protocol potentially available. The actual number of participants that participated in the [1-^{13}C]glycine infusion protocol, approximately one-half a year after the first, was 6.

Results

All participants (3 male, 3 female, age 21–26 y) had a BMI < 25 kg/m^2. Their serum folate, vitamin B-12, and plasma PLP concentrations were in the normal range and their plasma total homocysteine (<12 μmol/L) indicated normal 1-carbon metabolism and adequate nutritional status at each infusion protocol (**Table 1**).

In vivo rates of whole-body glycine and leucine turnover were nearly identical in both tracer protocols (**Table 2**), which indicates high reproducibility and comparability between the protocols using differently labeled glycine tracers. The plasma enrichment of the infused amino acid tracers is illustrated (**Fig. 2**).

Infusion of [1,2-^{13}C]glycine tracer yielded a significantly higher glycine-to-CO_2 flux than the [1-^{13}C]glycine tracer (Table 2). Glycine-to-CO_2 flux after infusion with [1-^{13}C]glycine indicated that GCS accounted for 22 ± 3% of whole-body glycine flux. The difference of glycine-to-CO_2 flux from [1,2-^{13}C]glycine vs. [1-^{13}C]glycine tracer implies a rate of CO_2 formation from the glycine 2-carbon of 51 ± 40 μmol·h^{-1}·kg^{-1}, which accounts for ~35% of the CO_2 generated in glycine catabolism. The AUC for breath $^{13}CO_2$ enrichment (**Fig. 3**) and the rate of $^{13}CO_2$ production ($V^{13}CO_2$) was significantly higher from the [1,2-^{13}C]glycine infusion compared with that of [1-^{13}C]glycine tracer (**Table 3**).

Discussion

Glycine is catabolized through the mitochondrial GCS and its 2-carbon is accepted by THF entering the folate cycle as methyleneTHF. The metabolic importance of this glycine cleavage reaction is illustrated by severe clinical symptoms, e.g. lethargy, apnea, seizures, and cognitive impairment in patients with loss-of-function mutations for genes encoding the components of the GCS. In these inborn errors, glycine accumulates to pathologic concentrations in cerebrospinal fluid and plasma leading to the conditions of nonketotic hyperglycinemia or glycine encephalopathy (19,20).

In the present study, 2 stable isotope tracer protocols were designed to quantify the rate of CO_2 generation from infused glycine to evaluate more extensively the quantitative role of glycine cleavage in folate-dependent 1-carbon metabolism and whole-body glycine metabolism. The use of both single- and double-labeled glycine tracers allowed a selective assessment of the relative fates of glycine carbons in CO_2 generation. Glycine is decarboxylated in the mitochondrial GCS, which accounted for 22% of the whole-body glycine flux. In addition to glycine decarboxylation via GCS, the 1-carbon of glycine can be released as CO_2 by pyruvate dehydrogenase and in the TCA cycle (Fig. 1). These reactions might have contributed partially to $^{13}CO_2$ formation after labeled glycine infusion. However, the activity of serine dehydratase forming pyruvate is lower in humans than other mammalian species (21) and, thus, pyruvate oxidation would contribute minimally to CO_2 formation from glycine. Further, because glycine is the direct substrate for GCS, we propose that CO_2 formation through the GCS would be substantially faster and quantitatively greater than from pyruvate dehydrogenase or the TCA cycle.

The results of this study also indicate that the formation of CO_2 from the glycine 2-carbon accounts for ~35% of the total CO_2 generation in glycine metabolism. The 2-carbon of glycine can be released as CO_2 by 10-formylTHF dehydrogenase and in

TABLE 1 Variables related to 1-carbon metabolism and body weight of healthy men and women prior to each infusion protocol[1]

	Protocol [1,2-^{13}C]glycine	Protocol [1-^{13}C]glycine
Plasma PLP, *nmol/L*	55 ± 9	63 ± 15
Serum folate, *nmol/L*	29 ± 8	28 ± 3
Serum vitamin B-12, *pmol/L*	395 ± 74	363 ± 80
Plasma tHcy,[2] *μmol/L*	7.9 ± 1.5	7.5 ± 1.5
Body weight, *kg*	69 ± 11	70 ± 13

[1] Values are mean ± SD, $n = 6$.
[2] tHcy, total homocysteine.

TABLE 2 Plateau enrichment of stable isotope-labeled amino acids and their metabolic products and the corresponding flux values after infusion with [1,2-^{13}C]glycine or [1-^{13}C]glycine and [$^2H_3$]leucine[1]

	Protocol [1,2-^{13}C]glycine		Protocol [1-^{13}C]glycine	
	Ep, *mol % excess*	Whole-body Q, *μmol·h^{-1}·kg^{-1}*	Ep, *mol % excess*	Whole-body Q, *μmol·h^{-1}·kg^{-1}*
Infused AA		$Q_{infused\ AA}$		$Q_{infused\ AA}$
[$^2H_3$]leucine	1.69 ± 0.15	109 ± 11	1.86 ± 0.11	99 ± 6
[$^{13}C_2$]glycine	5.54 ± 1.26	423 ± 79	5.36 ± 0.78	430 ± 62
CO_2 generation		$Q_{Gly \rightarrow CO2}$		$Q_{Gly \rightarrow CO2}$
[$^{13}CO_2$]	0.046 ± 0.006	146 ± 37	0.033 ± 0.003*	96 ± 8‡

[1] Values are mean ± SD, $n = 6$. Symbols indicate different from [1,2-^{13}C]glycine protocol: *$P = 0.0003$; ‡$P = 0.026$ (paired *t* test). AA, amino acids.

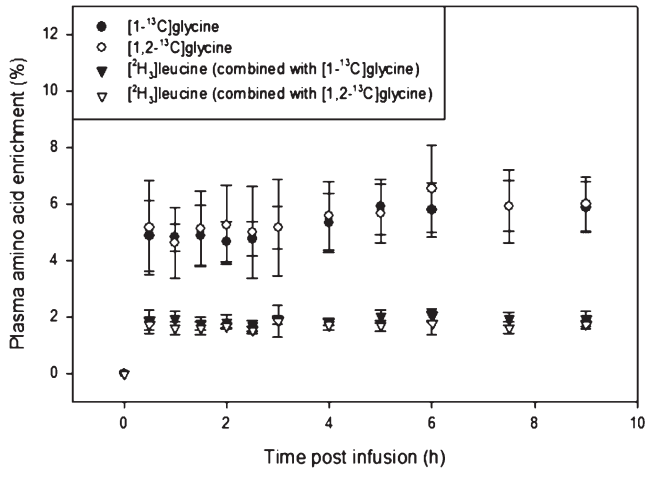

FIGURE 2 Plasma enrichment of infused amino acids in healthy men and women during primed, constant infusion with 9.26 μmol·kg^{-1}·h^{-1} [1,2-^{13}C]glycine or 9.26 μmol·kg^{-1}·h^{-1} [1-^{13}C]glycine and 1.87 μmol·kg^{-1}·h^{-1} [$^2H_3$]leucine. Values are means ± SEM, $n = 6$.

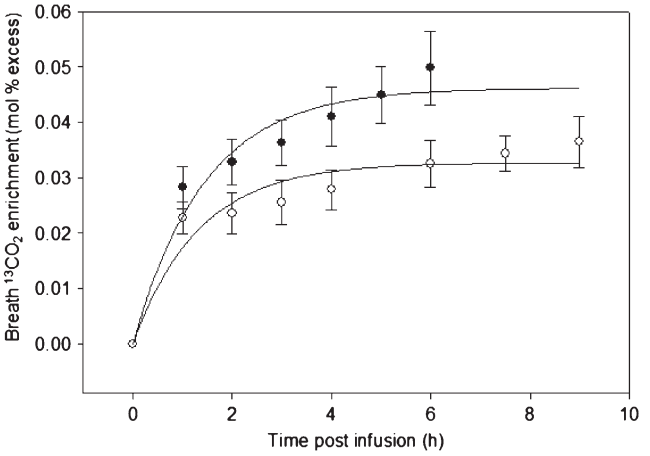

FIGURE 3 Breath $^{13}CO_2$ enrichment in healthy men and women during primed, constant infusion with [1,2-^{13}C]glycine (closed circles) or [1-^{13}C]glycine (open circles). Values are means ± SEM, $n = 6$.

the TCA cycle. The TCA cycle is further downstream in the metabolism where the isotopic enrichment of oxaloacetate and other TCA cycle constituents become increasingly diluted. We therefore speculate that the $^{13}CO_2$ enrichment of TCA cycle components would be very low. If this assumption is true, it appears that $^{13}CO_2$ formation from the glycine 2-carbon occurs primarily from the conversion of 10-formylTHF to THF and CO_2 by 10-formylTHF dehydrogenase. Recent mathematical modeling predicted that 10-formylTHF dehydrogenase would contribute to CO_2 generation at a rate of ~30% of the rate of GCS in hepatic metabolism (22). This study appears to represent, to our knowledge, the first in vivo evaluation of 10-formylTHF dehydrogenase flux with a rate of ~51 μmol·h^{-1}·kg^{-1}. The rate of CO_2 formation from the glycine 2-carbon greatly varied among participants. 10-FormylTHF dehydrogenase was reported to be downregulated in tumor tissues (23), but the basis of its regulation in healthy adults and factors responsible for interindividual variation is unclear. The physiologic significance of variability in whole-body 10-formylTHF dehydrogenase flux needs further investigations.

The mean glycine cleavage rate of 96 μmol·h^{-1}·kg^{-1} implies that GCS produces methyleneTHF at a very high rate for use in folate-dependent 1-carbon metabolism. To put this into the context of overall demand for 1-carbon units, total homocysteine remethylation flux employs 5-methylTHF (derived from methyleneTHF) as the 1-carbon donor at a rate of 2–8 μmol·h^{-1}·kg^{-1} (14). These results provide clear evidence that the GCS produces 1-carbon units as methyleneTHF at a rate of ~20 times that needed for homocysteine remethylation and, thus, for methylation demand. In patients with nonketotic hyperglycinemia, the elevated homocysteine concentration in cerebrospinal fluid might indicate a lack of GCS-derived 1-carbon units for homocysteine remethylation (24). The high rate of methyleneTHF production from glycine cleavage suggests that the GCS might supply methyleneTHF in support of a very high flux of purine and thymidylate synthesis. However, this hypothesis appears to be incorrect. In the [1,2-^{13}C]glycine infusion protocol, the incorporation of GCS-derived methyleneTHF in serine synthesis via SHMT occurred at a rate of ~92 μmol·kg^{-1}·h^{-1} (7). In comparison, the [1-^{13}C]glycine tracer indicated that the GCS reaction occurred at a whole-body rate of 96 μmol·kg^{-1}·h^{-1}. We conclude that nearly all GCS-derived 1-carbon units are consumed in serine synthesis while a much smaller percentage enters all other aspects of 1-carbon metabolism, including nucleoside synthesis, homocysteine remethylation, and *S*-adenosylmethionine-dependent methylation reactions (7). We acknowledge that this conclusion is based on whole-body flux measurements. The contribution of glycine to nucleoside synthesis and methylation reactions is likely to be cell-type or tissue-specific and cannot be determined with the present stable isotope tracer protocol. The quantitative role of glycine in providing 1-carbon units for nucleotide synthesis and the quantitative role of serine synthesis in gluconeogenesis need further investigation.

TABLE 3 AUC of breath $^{13}CO_2$ enrichment and V$^{13}CO_2$ after infusion with [1,2-^{13}C]glycine or [1-^{13}C]glycine and [$^2H_3$]leucine[1]

	Protocol [1,2-^{13}C]glycine	Protocol [1-^{13}C]glycine	Difference
AUC of $^{13}CO_2$ enrichment, *mol % excess over 6 h*	0.0347 ± 0.0041	0.0244 ± 0.0032	0.0103 ± 0.0034*
AUC of V$^{13}CO_2$, *μmol·h^{-1}·kg^{-1} over 6 h*	2.46 ± 0.52	1.62 ± 0.23	0.84 ± 0.65‡
VCO_2, *μmol·h^{-1}·kg^{-1}*	5383 ± 460	5772 ± 678	

[1] Values are mean ± SD, $n = 6$. Symbols indicate difference: *$P < 0.001$; ‡$P = 0.025$ (2-sided paired *t* test).

The recently published protocol using [1,2-^{13}C]glycine tracer infusion (7) was designed for quantification of whole-body glycine flux, rate of glycine cleavage, serine synthesis rate, and contribution of glycine in nucleoside synthesis (7). We recognized the potential for overestimation of GCS flux because of the smaller but not inconsequential generation of CO_2 from the glycine 2-carbon. The present study provides further insight regarding the interpretation of the quantitative aspects of glycine catabolism and the role of glycine in 1-carbon metabolism. We conclude from this kinetic analysis that the total rate of glycine decarboxylation is ~30–35% less than the estimate based on total $^{13}CO_2$ generation from [1,2-^{13}C]glycine tracer infusion protocol reported here and in our previous article (7).

These tracer protocols were performed in participants in the fed state to accelerate pathways by substrate loads (11). Whole-body glycine turnover was ~430 μmol·h^{-1}·kg^{-1} in these healthy men and women. This is consistent with a glycine flux of 458 μmol·h^{-1}·kg^{-1}, as determined by Gersovitz (25) also in fed participants. Robert et al. (18) measured a glycine flux of 240 μmol·h^{-1}·kg^{-1} in young, healthy men who were fasting. Other influencing factors on amino acid flux and their metabolic pathways are hormonal variations, e.g. glucagon levels. In rat hepatocytes, glucagon activated GCS by a phosphorylation-mediated cell-signaling mechanism (26,27).

In conclusion, the results of this study provide evidence for and quantitative insight into the major role of glycine and the mitochondrial GCS as a source of methyleneTHF 1-carbon units for supplying serine synthesis and folate-dependent 1-carbon metabolism. We have recently reported that mild vitamin B-6 restriction has little effect on GCS flux in healthy adults (7). In view of its quantitative importance in human metabolism, other aspects of physiological, genetic, and nutritional regulation of the GCS in health and disease should be evaluated.

Literature Cited

1. Kikuchi G. The glycine cleavage system: composition, reaction mechanism, and physiological significance. Mol Cell Biochem. 1973;1:169–87.

2. Bailey LB, Gregory JF III. Folate metabolism and requirements. J Nutr. 1999;129:779–82.
3. Garcia-Martinez LF, Appling DR. Characterization of the folate-dependent mitochondrial oxidation of carbon 3 of serine. Biochemistry. 1993;32:4671–6.
4. Lamers Y, Williamson J, Gilbert LR, Stacpoole PW, Gregory JF III. Glycine turnover and decarboxylation rate quantified in healthy men and women using primed, constant infusions of [1,2-$^{13}C_2$]glycine and [$^{2}H_3$]leucine. J Nutr. 2007;137:2647–52.
5. Cuskelly GJ, Stacpoole PW, Williamson J, Baumgartner TG, Gregory JF III. Deficiencies of folate and vitamin B(6) exert distinct effects on homocysteine, serine, and methionine kinetics. Am J Physiol Endocrinol Metab. 2001;281:E1182–90.
6. Davis SR, Stacpoole PW, Williamson J, Kick LS, Quinlivan EP, Coats BS, Shane B, Bailey LB, Gregory JF III. Tracer-derived total and folate-dependent homocysteine remethylation and synthesis rates in humans indicate that serine is the main one-carbon donor. Am J Physiol Endocrinol Metab. 2004;286:E272–9. Erratum in Am J Physiol Endocrinol Metab 2004;286:E674.
7. Lamers Y, Williamson J, Ralat M, Quinlivan EP, Gilbert LR, Keeling C, Stevens RD, Newgard CB, Ueland PM, et al. Moderate dietary vitamin B-6 restriction raises plasma glycine and cystathionine concentrations while minimally affecting the rates of glycine turnover and glycine cleavage in healthy men and women. J Nutr. 2009;139:452–60.
8. Parra MD, Martinez JA. Nutritional aspects of breath testing based on stable isotopes. Nutr Rev. 2006;64:338–47.
9. Ubbink JB, Serfontein WJ, de Villiers LS. Stability of pyridoxal-5-phosphate semicarbazone: applications in plasma vitamin B6 analysis and population surveys of vitamin B6 nutritional status. J Chromatogr. 1985;342:277–84.
10. Pfeiffer CM, Huff DL, Gunter EW. Rapid and accurate HPLC assay for plasma total homocysteine and cysteine in a clinical laboratory setting. Clin Chem. 1999;45:290–2.
11. Storch KJ, Wagner DA, Burke JF, Young VR. Quantitative study in vivo of methionine cycle in humans using [methyl-$^{2}H_3$]- and [1-^{13}C]methionine. Am J Physiol. 1988;255:E322–31.
12. MacCoss MJ, Fukagawa NK, Matthews DE. Measurement of intracellular sulfur amino acid metabolism in humans. Am J Physiol Endocrinol Metab. 2001;280:E947–55.
13. Wolfe RR. Radioactive and stable isotope tracers in biomedicine: principles and practice of kinetic analysis. New York: Wiley Liss; 1992.
14. Davis SR, Scheer JB, Quinlivan EP, Coats BS, Stacpoole PW, Gregory JF III. Dietary vitamin B-6 restriction does not alter rates of homocysteine remethylation or synthesis in healthy young women and men. Am J Clin Nutr. 2005;81:648–55.
15. Gregory JF III, Cuskelly GJ, Shane B, Toth JP, Baumgartner TG, Stacpoole PW. Primed, constant infusion with [$^{2}H_3$]serine allows in vivo kinetic measurement of serine turnover, homocysteine remethylation, and transsulfuration processes in human one-carbon metabolism. Am J Clin Nutr. 2000;72:1535–41.
16. Arends J, Schafer G, Schauder P, Bircher J, Bier DM. Comparison of serine and hippurate as precursor equivalents during infusion of [^{15}N]glycine for measurement of fractional synthetic rates of apolipoprotein B of very-low-density lipoprotein. Metabolism. 1995;44:1253–8.
17. Cryer DR, Matsushima T, Marsh JB, Yudkoff M, Coates PM, Cortner JA. Direct measurement of apolipoprotein B synthesis in human very low density lipoprotein using stable isotopes and mass spectrometry. J Lipid Res. 1986;27:508–16.
18. Robert JJ, Bier DM, Zhao XH, Matthews DE, Young VR. Glucose and insulin effects on the novo amino acid synthesis in young men: studies with stable isotope labeled alanine, glycine, leucine, and lysine. Metabolism. 1982;31:1210–8.
19. Hiraga K, Kochi H, Hayasaka K, Kikuchi G, Nyhan WL. Defective glycine cleavage system in nonketotic hyperglycinemia. Occurrence of a less active glycine decarboxylase and an abnormal aminomethyl carrier protein. J Clin Invest. 1981;68:525–34.
20. Pearl PL, Capp PK, Novotny EJ, Gibson KM. Inherited disorders of neurotransmitters in children and adults. Clin Biochem. 2005;38:1051–8.
21. Xue HH, Sakaguchi T, Fujie M, Ogawa H, Ichiyama A. Flux of the L-serine metabolism in rabbit, human, and dog livers. Substantial contributions of both mitochondrial and peroxisomal serine:pyruvate/alanine:glyoxylate aminotransferase. J Biol Chem. 1999;274:16028–33.
22. Nijhout HF, Reed MC, Lam SL, Shane B, Gregory JF III, Ulrich CM. In silico experimentation with a model of hepatic mitochondrial folate metabolism. Theor Biol Med Model. 2006;3:40.
23. Krupenko SA, Oleinik NV. 10-Formyltetrahydrofolate dehydrogenase, one of the major folate enzymes, is down-regulated in tumor tissues and possesses suppressor effects on cancer cells. Cell Growth Differ. 2002;13:227–36.
24. Van Hove JL, Lazeyras F, Zeisel SH, Bottiglieri T, Hyland K, Charles HC, Gray L, Jaeken J, Kahler SG. One-methyl group metabolism in non-ketotic hyperglycinaemia: mildly elevated cerebrospinal fluid homocysteine levels. J Inherit Metab Dis. 1998;21:799–811.
25. Gersovitz M, Bier D, Matthews D, Udall J, Munro HN, Young VR. Dynamic aspects of whole body glycine metabolism: influence of protein intake in young adult and elderly males. Metabolism. 1980;29:1087–94.
26. Jois M, Hall B, Brosnan JT. Stimulation of glycine catabolism in isolated perfused rat liver by calcium mobilizing hormones and in isolated rat liver mitochondria by submicromolar concentrations of calcium. J Biol Chem. 1990;265:1246–8.
27. Jois M, Hall B, Fewer K, Brosnan JT. Regulation of hepatic glycine catabolism by glucagon. J Biol Chem. 1989;264:3347–51.